

RESEARCH ARTICLE

Mapping Variation in Cellular and Transcriptional Response to 1,25-Dihydroxyvitamin D3 in Peripheral Blood Mononuclear Cells

Silvia N. Kariuki¹, Joseph C. Maranville^{1¶a}, Shaneen S. Baxter^{1¶b}, Choongwon Jeong¹, Shigeki Nakagome¹, Cara L. Hrusch², David B. Witonsky¹, Anne I. Sperling², Anna Di Rienzo^{1*}

1 Department of Human Genetics, University of Chicago, Chicago, Illinois, United States of America,

2 Department of Medicine, University of Chicago, Chicago, Illinois, United States of America

¶a Current address: Merck Research Labs, Boston, Massachusetts, United States of America

¶b Current address: Center for Vascular and Inflammatory Diseases, University of Maryland School of Medicine, Baltimore, Maryland, United States of America

* dirienzo@bsd.uchicago.edu



OPEN ACCESS

Citation: Kariuki SN, Maranville JC, Baxter SS, Jeong C, Nakagome S, Hrusch CL, et al. (2016) Mapping Variation in Cellular and Transcriptional Response to 1,25-Dihydroxyvitamin D3 in Peripheral Blood Mononuclear Cells. PLoS ONE 11(7): e0159779. doi:10.1371/journal.pone.0159779

Editor: Pratibha V. Nerurkar, College of Tropical Agriculture and Human Resources, University of Hawaii, UNITED STATES

Received: March 16, 2016

Accepted: July 6, 2016

Published: July 25, 2016

Copyright: © 2016 Kariuki et al. This is an open access article distributed under the terms of the [Creative Commons Attribution License](https://creativecommons.org/licenses/by/4.0/), which permits unrestricted use, distribution, and reproduction in any medium, provided the original author and source are credited.

Data Availability Statement: The microarray data have been deposited in the Gene Expression Omnibus (GEO) under accession number GSE82023. In addition, reviewers can access the data on the following link: <http://www.ncbi.nlm.nih.gov/geo/query/acc.cgi?token=uhijawekrfenpmz&acc=GSE82023>.

Funding: This work was supported in part by NIH grant (R01 GM101682) to ADR. SNK was supported by a Howard Hughes Medical Institute Gilliam Fellowship for Advanced Study. CJ was supported by

Abstract

The active hormonal form of vitamin D, 1,25-dihydroxyvitamin D (1,25D) is an important modulator of the immune system, inhibiting cellular proliferation and regulating transcription of immune response genes. In order to characterize the genetic basis of variation in the immunomodulatory effects of 1,25D, we mapped quantitative traits of 1,25D response at both the cellular and the transcriptional level. We carried out a genome-wide association scan of percent inhibition of cell proliferation (I_{max}) induced by 1,25D treatment of peripheral blood mononuclear cells from 88 healthy African-American individuals. Two genome-wide significant variants were identified: rs1893662 in a gene desert on chromosome 18 ($p = 2.32 \times 10^{-8}$) and rs6451692 on chromosome 5 ($p = 2.55 \times 10^{-8}$), which may influence the anti-proliferative activity of 1,25D by regulating the expression of nearby genes such as the chemokine gene, *CCL28*, and the translation initiation gene, *PAIP1*. We also identified 8 expression quantitative trait loci at a $FDR < 0.10$ for transcriptional response to 1,25D treatment, which include the transcriptional regulator ets variant 3-like (*ETV3L*) and EH-domain containing 4 (*EHD4*). In addition, we identified response eQTLs in vitamin D receptor binding sites near genes differentially expressed in response to 1,25D, such as FERM Domain Containing 6 (*FRMD6*), which plays a critical role in regulating both cell proliferation and apoptosis. Combining information from the GWAS of I_{max} and the response eQTL mapping enabled identification of putative I_{max} -associated candidate genes such as *PAIP1* and the transcriptional repressor gene *ZNF649*. Overall, the variants identified in this study are strong candidates for immune traits and diseases linked to vitamin D, such as multiple sclerosis.

a Samsung Scholarship for post-graduate overseas education of Korean nationals. This project was supported by the University of Chicago Comprehensive Cancer Center Support Grant (#P30 CA14599), with particular support from the Genomics Core Facility. The Center for Research Informatics is funded by the Biological Sciences Division at the University of Chicago with additional funding provided by the Institute for Translational Medicine, CTSA grant number UL1 TR000430 from the National Institutes of Health. The funders had no role in study design, data collection and analysis, decision to publish, or preparation of the manuscript.

Competing Interests: The authors have declared that no competing interests exist.

Introduction

Epidemiological studies have linked variation in the circulating inactive form of vitamin D, 25-hydroxyvitamin D₃ (25D), to risk of autoimmune diseases such as multiple sclerosis, type 1 diabetes and systemic lupus erythematosus [1–7], consistent with the known effects of vitamin D as an immune system modulator [8–12]. Furthermore, genetic variation in the vitamin D pathway is linked to autoimmune disease risk. For example, several studies have highlighted associations between variants in *CYP27B1*, which encodes the enzyme that activates 25D to 1,25-dihydroxyvitamin D₃ (1,25D), and risk for multiple sclerosis [13–15].

The fact that immune cells express *CYP27B1* indicates that active vitamin D can be produced intra-cellularly in the immune system in response to organismal demands such as infections. Immune cells also express the vitamin D receptor (VDR), which when bound by the active 1,25D, forms a heterodimer with the retinoid X receptor (RXR) and translocates to the nucleus, resulting in transcriptional regulation of vitamin D-responsive genes [8, 9, 11, 12, 16]. The genes regulated by 1,25D are involved in various pathways including metabolic regulation, antimicrobial response and inflammatory cytokine response [7, 17–23].

Extensive inter-individual and inter-ethnic variation in the circulating levels of 25D levels has been reported, with lower levels on average in African Americans compared to European Americans [24–27]. These differences are known to be influenced by various factors such as sun exposure, dietary intake, as well as genetic variations in critical genes in the vitamin D metabolic pathway [14, 28, 29]. Despite the strong epidemiological associations of 25D levels and disease risk, randomized clinical trials aimed at testing the efficacy of vitamin D supplementation as a therapeutic intervention [4, 17, 30–34] have yielded mixed results [35, 36]. In addition to environmental confounders, these results could be due to inter-individual differences in the response to vitamin D, irrespective of its concentration in circulation or within the cells at the level of the target organ. Indeed, at least one study identified a polymorphism in the *VDR* gene that influenced the response to vitamin D supplementation [37]. However, beyond the *VDR* gene, little—if anything—is known about the contribution of genetics to the inter-individual variation in response to vitamin D.

The aim of this study was to map the genetic bases of inter-individual variation in the transcriptional response to 1,25D and in the inhibition of cell proliferation induced by 1,25D in primary peripheral blood mononuclear cells (PBMCs) obtained from African-American healthy individuals. We primarily focused on African-American individuals as epidemiological data indicate that they have a higher proportion of 25D deficiency, and should hence be considered prime targets of supplementation studies, which in turn could benefit from knowledge of genetic variation affecting response to supplementation. Moreover, measuring the proportion of genome-wide African ancestry enabled us to test the relationship between African ancestry proportions and response to 1,25D within the same ethnic group. To isolate the effects of genetic variation on the response to active vitamin D rather than on its concentration, we treated PBMCs cultured *in vitro* with a fixed amount of 1,25D and, in parallel, with a vehicle control. This allowed us to characterize the response to vitamin D both at the cellular and transcriptional level and to identify genetic variants associated with cellular and transcriptional response to 1,25D. Moreover, by measuring the proportion of African ancestry in the African-American cohort in this study, we were able to directly test the relationship between African ancestry and response to 1,25D.

Methods

Samples

Peripheral blood was obtained from 88 African American (AA) donors collected by Research Blood Components (<http://researchbloodcomponents.com/>) as part of a larger study on

transcriptional response [38]. All subjects were healthy donors and were not on any medication. All donors to Research Blood Components are required to sign an Institutional Review Board (IRB)-approved consent form giving permission to collect blood, and use it for research purposes. The IRB at the University of Chicago determined that this study is not human subjects research because blood samples were not shipped with individually identifiable information. Self-reported ethnicity, age, gender, date, and time of blood drawing were recorded for each donor (S1 Table). Samples were processed in multiple successive batches. Batch number was recorded and used as a covariate.

Cell Culture and Treatment

The experimental design is illustrated in S1 Fig. We isolated peripheral blood mononuclear cells (PBMCs) from heparin-treated whole blood by density gradient centrifugation using Ficoll-Paque PLUS medium (GE Healthcare Life Sciences, Pittsburgh, PA), within 24 hours of blood draw for all the samples. PBMCs were washed in PBS and transferred to RPMI supplemented with 10% charcoal-stripped fetal bovine serum. Each sample was then divided into one aliquot of 1.8×10^6 cells for measuring cell proliferation, and one aliquot of 9×10^6 cells for genome-wide transcriptional profiling. For the cell proliferation measurements, PBMCs were cultured at 2×10^5 cells per well in 10% charcoal-stripped media in 96-well plates. Each donor was treated in triplicate with phytohemagglutinin (PHA) (2.5ug/ml) and either vehicle (EtOH) or 1,25-dihydroxyvitamin D3 (1,25D) (100nM) for 48 hours [38, 39]. For transcriptional profile measurements, PBMCs from each donor were cultured at 10^6 cells per well in 10% charcoal-stripped media in 24-well plates. As with the cellular proliferation measurements, each donor was treated in triplicate with PHA (2.5ug/ml) and either vehicle or 1,25D (100nM) for 6 hours. Since the mechanism of action of 1,25D is primarily transcriptional, the effects of 1,25D on cell proliferation are expected to be downstream to the transcriptional effects, hence, we chose a shorter time for the transcriptional response compared to the longer time point for cell proliferation. In addition, a strong transcriptional response to 1,25D in PBMCs had been observed at a similar time point in a previous study from our group; none of the subjects from the previous study were included here [39]. Cell type composition of the PBMCs was measured using flow cytometry as previously reported for these samples [38], where proportions of T cells including T helper cells (CD4⁺) and cytotoxic T (CD8⁺) cells, B cells, monocytes and neutrophils were measured using antibodies specifically targeting these cell types. The cell type composition and other sample characteristics are summarized in S1 Table.

Cellular Proliferation Measurements

After 48 hours of treatment, cell proliferation was measured by H³-thymidine incorporation using standard protocols as previously described [38–40]. Briefly, proliferation measurements, obtained from the counts per minute (CPM) values of the thymidine incorporation assay, were obtained for each treatment (1,25D+PHA or vehicle+PHA). The median CPM values were taken from across the three replicates. Percent inhibition of proliferation by 1,25D (I_{\max}) was calculated as $1 - [(\text{proliferation in } 1,25\text{D}+\text{PHA})/(\text{proliferation in EtOH}+\text{PHA})]$, and fit to a normal distribution. The median CPM values for each treatment across all samples, and the corresponding I_{\max} values are listed in S2 Table. Associations between covariates and I_{\max} were tested using a simple linear regression.

Transcriptional Response Profiling

After 6 hours of treatment with PHA and 1,25D or vehicle, the three replicates from each donor were pooled before RNA extraction. Total RNA was extracted from each pool with the

RNeasy Plus Mini Kit (Qiagen 74134). Total RNA was reverse transcribed into cDNA, labeled, hybridized to Illumina (San Diego, CA, USA) Human HT-12 v3 Expression Beadchips and scanned at the University of Chicago Functional Genomics Core facility. We performed low-level microarray analyses using the Bioconductor software package LUMI [41] in R, as previously described [40]. Briefly, we annotated probes by mapping their sequence to RefSeq (GRCh37) transcripts using BLAT. We discarded probes that mapped to multiple genes, or contained one or more HapMap SNPs. We applied variance stabilization transformation to all arrays, discarded poor quality probes, and quantile normalized the arrays using the default method implemented in the lumiN function. After these filters, probes mapping to 11,897 genes were used in downstream analyses. The normalized gene expression values are available in [S3 Table](#). We used a paired t-test to identify genes that were differentially expressed between 1,25D- and vehicle-treated samples. The results from the paired t-test analysis for all 11,897 genes are available in [S3 Table](#). False-discovery rates (FDR) were estimated using the q value function in R [42]. Gene set enrichment analysis was performed using the commercially available software Ingenuity Pathway Analysis (IPA).

Genome-Wide Association of Inhibition of Cellular Proliferation by 1,25D (I_{\max})

Samples were genotyped on two Illumina Omni BeadChip platforms, with a total of 884,015 SNPs across the genome genotyped for each donor, as previously described [38]. We then imputed genotypes at all SNPs identified in the 1000 Genomes Project [43] using IMPUTE2 [44], applying the output file flag option “-pgs_miss”, which replaces the missing genotypes at typed SNPs with imputed genotypes. We filtered SNPs for minor allele frequency (>0.1), imputation quality (>0.9), and departure from Hardy Weinberg equilibrium ($p > 0.001$), resulting in a total of 4,047,158 SNPs available for all 88 samples.

We performed a genome-wide association scan (GWAS) of the cellular inhibition of proliferation by 1,25D (I_{\max}) using a likelihood ratio test correcting for genome-wide proportions of African ancestry to control for spurious associations due to population structure. Genome-wide African ancestry proportions in each donor were estimated using STRUCTURE which uses multi-locus genotype data to investigate the genetic structure of populations [45]. Prior to the GWAS analysis, I_{\max} was corrected for all covariates including age, gender, and cell type proportions.

Mapping Variation in Transcriptional Response

We performed a genome-wide test for association between \log_2 fold change at every gene and SNPs within 100kb of the transcriptional start site of each gene. Transcriptional response profile data was not collected for 3 out of the 88 donors. For the 85 donors, the total number of genome-wide SNPs available for eQTL mapping that passed the filters described earlier was 4,100,242. eQTL mapping was performed using Matrix eQTL software, which performs a linear regression test for association between each SNP and each transcript, modeling the additive linear genotype effect on transcriptional response [46]. FDRs were calculated according to the Benjamini and Hochberg method [47]. We also corrected for genome-wide African ancestry proportions in this analysis.

As a complementary approach, we applied a Bayesian statistical framework that identifies different genotype-treatment interaction patterns, using the statistical software BRIDGE [48]. We mapped interaction eQTLs within 100kb of expressed genes, modeling four conditions through which SNPs could interact with transcriptional response phenotype under the two treatment conditions (1,25D and control): (i) Control-only model, where genotype is associated with transcript levels in control-treated aliquots, but not in 1,25D-treated aliquots, (ii)

1,25D-only model, where genotype is associated with transcript levels in 1,25D-treated aliquots, but not in EtOH-treated aliquots, (iii) General interaction model, where genotype is associated with transcript levels in both conditions, but with different effects in each condition, and (iv) No interaction model, where genotype is associated with transcript levels in both conditions, with equal effect in each condition (baseline eQTLs). Using a hierarchical model, information across SNPs in each gene region and across genes was combined, and a posterior probability for each gene that it follows each of the models, and that it is affected by a SNP that follows that model, was calculated.

Identifying eQTLs within Regulatory Regions

We reanalyzed published data sets of VDR ChIP-seq obtained in THP-1 monocytic cell lines treated with 1,25D and LPS or 1,25D alone [49], and FAIRE-seq performed in THP-1 cells treated with 1,25D [50]. First, we aligned sequence reads to the human reference (GRCh37) using BWA backtrack 0.7.5. Second, we kept only sequence reads with phred-scaled mapping quality ≥ 30 using samtools v1.1 [51]. Third, PCR duplicate were removed with picard tool v 1.130 (<http://broadinstitute.github.io/picard/>). For the ChIP-seq data sets, we confirmed the quality of data sets by strand cross-correlation (SCC) analysis [52] implemented in the R script “run_spp_nodups.R” packaged in phantompeakqualtools (<https://code.google.com/p/phantompeakqualtools/>). Statistically significant peaks were identified using MACS version 2 [53] with the following essential command line arguments: `macs2 callpeak—bw X -g hs—qvalue = 0.05 -m 5 50`, where X is a length of the bandwidth that was defined as a fragment length calculated by SCC for the ChIP-seq data or as 200 bp for the FAIRE-seq data reported in Seuter *et al.* (2012).

Out of the 4,100,242 SNPs available for eQTL mapping, we identified subsets of these SNPs that were within ChIP-seq and FAIRE-seq peaks. We then used these subsets of SNPs to map response eQTLs using Matrix eQTL as described in the previous section.

Overlap between Cellular and Transcriptional Response Phenotypes

To identify genes whose transcriptional response to 1,25D may play a role in the inhibition of cell proliferation, we performed linear regression to test the association across individuals between the cellular response phenotype (I_{\max}), and log-fold change response (1,25D-treated over vehicle-treated expression), and we estimated FDR using the q value function in R. We also applied a Bayesian method with the program Sherlock [54] to predict putative causal genes associated with I_{\max} . This method predicts causal genes by identifying SNPs in these genes that are associated both with gene expression in *cis* and *trans*, and with the trait of interest, in our case, I_{\max} . We used the results from the response *cis*-eQTL mapping and the GWAS of I_{\max} to perform this analysis, setting the prior for association of each SNP with gene expression in *cis*, as well as association of each SNP with I_{\max} , to 0.01. We chose this high prior due to the fact that we were examining transcriptional and cellular response phenotypes in primary cells obtained from the same individuals. The statistical significance of the Bayes factor for each gene was indicated by the corresponding p-values, which were calculated by permutation of the GWAS data, as detailed by He *et al.* (2013).

Results

Mapping Variation in Inhibition of Cellular Proliferation by 1,25D

To characterize inter-individual variation in cellular response to 1,25D, we measured cellular proliferation in PBMCs, which had been stimulated for 48 hours with PHA in the presence of

either 1,25D or its vehicle (EtOH) as a control. I_{\max} was calculated as the proportion of proliferation in 1,25D treated cells relative to proliferation in vehicle-treated cells. The average I_{\max} value across the 88 samples was 25%, with a maximum I_{\max} of 80%. Negative I_{\max} values were observed in some samples, where there was more proliferation after 1,25D treatment (S2 Table and S3 Fig).

Using a simple linear regression, we measured the association between each donor's age, gender, time of collection, batch, serum 25D and cortisol levels, and found no significant correlations between these covariates and I_{\max} . We also found no significant correlations between cell type proportions, as well as baseline levels of the vitamin D receptor gene (*VDR*), and I_{\max} (S4 Table). However, to avoid any potential sources of confounding, we corrected I_{\max} for all of these covariates before further downstream analyses.

To control for spurious associations potentially caused by population structure, we corrected for the proportion of genome-wide African ancestry in each donor, estimated using the program STRUCTURE. The median proportion of African ancestry in our donors was 81.4%, with an interquartile range of 14.7%. There were no significant correlations between I_{\max} or the other covariates, and proportion of African ancestry. However, there was a negative correlation between the genome-wide proportion of African ancestry and serum 25D levels ($p = 0.035$, $\beta = -0.034$) (S2 Fig), which suggests a genetic contribution to the higher prevalence of vitamin D insufficiency observed in African Americans [24]. The average serum 25D level in our African American donors was 20.81nM with a standard deviation of 10.39nM, which is a level considered to be at risk for deficiency according to the Institute of Medicine definitions (less than 30nM) [55].

To investigate the genetic bases of variation in I_{\max} , we carried out a genome-wide association scan for a total of 4,047,158 SNPs and identified genome-wide significant SNPs in chromosomes 5 and 18 (Fig 1A and 1B). The top signal of association was an intergenic SNP in chromosome 18 (rs1893662, $p = 2.32 \times 10^{-8}$) (Fig 1A and 1C, S5 Table). The A allele was associated with increased inhibition of proliferation (Fig 1E), and had a lower frequency in populations of African ancestry compared to European and Asian populations (allele frequency: 0.325, 0.811, and 0.648 respectively) (S4A Fig). The next strongest signal of association was an intergenic SNP in chromosome 5 (rs6451692, $p = 2.55 \times 10^{-8}$) (Fig 1A and 1D, S5 Table). The C allele was associated with increased inhibition of proliferation (Fig 1F), and had a higher frequency in populations of African ancestry compared to European and Asian populations (allele frequency: 0.839, 0.565, and 0.198 respectively) (S4B Fig). The closest gene to this SNP is *CCL28*, which encodes a chemokine that recruits T cells, eosinophils, and B cells to mucosal sites; other genes within 100 kb of this SNP are two uncharacterized open reading frames (*C5orf28* and *C5orf35*) and *PAIP1*, which plays a role in stimulating translation initiation. Interestingly, we observed a marginal association between rs6451692 C allele and transcriptional response of *PAIP1* to 1,25D ($p = 0.02$, $\beta = -0.39$) (S6 Table). In addition, this SNP lies less than 1 kb away from H3K4me1 enhancer-associated chromatin marks, DNase I hypersensitive sites and binding events for transcription factors such as TCF7L2, GATA3 and CEBPB in seven cell lines from the ENCODE project, including lymphoblastoid cell lines [56] (S5 Fig). These chromatin marks highlight the potential regulatory activity of rs6451692 on transcriptional activity in immune cells.

To determine the proportion of variation of I_{\max} explained by the top two SNPs in chromosomes 18 and 5, we examined the correlation coefficient from the linear model measuring the association between the top two associated SNPs and I_{\max} . These two SNPs had a large effect on I_{\max} , where rs1893662 explained 29.94% of the phenotypic variation in our samples, while rs6451692 explained 29.8% of the phenotypic variation in our samples. These top two SNPs explained ~45% of the variation in I_{\max} .

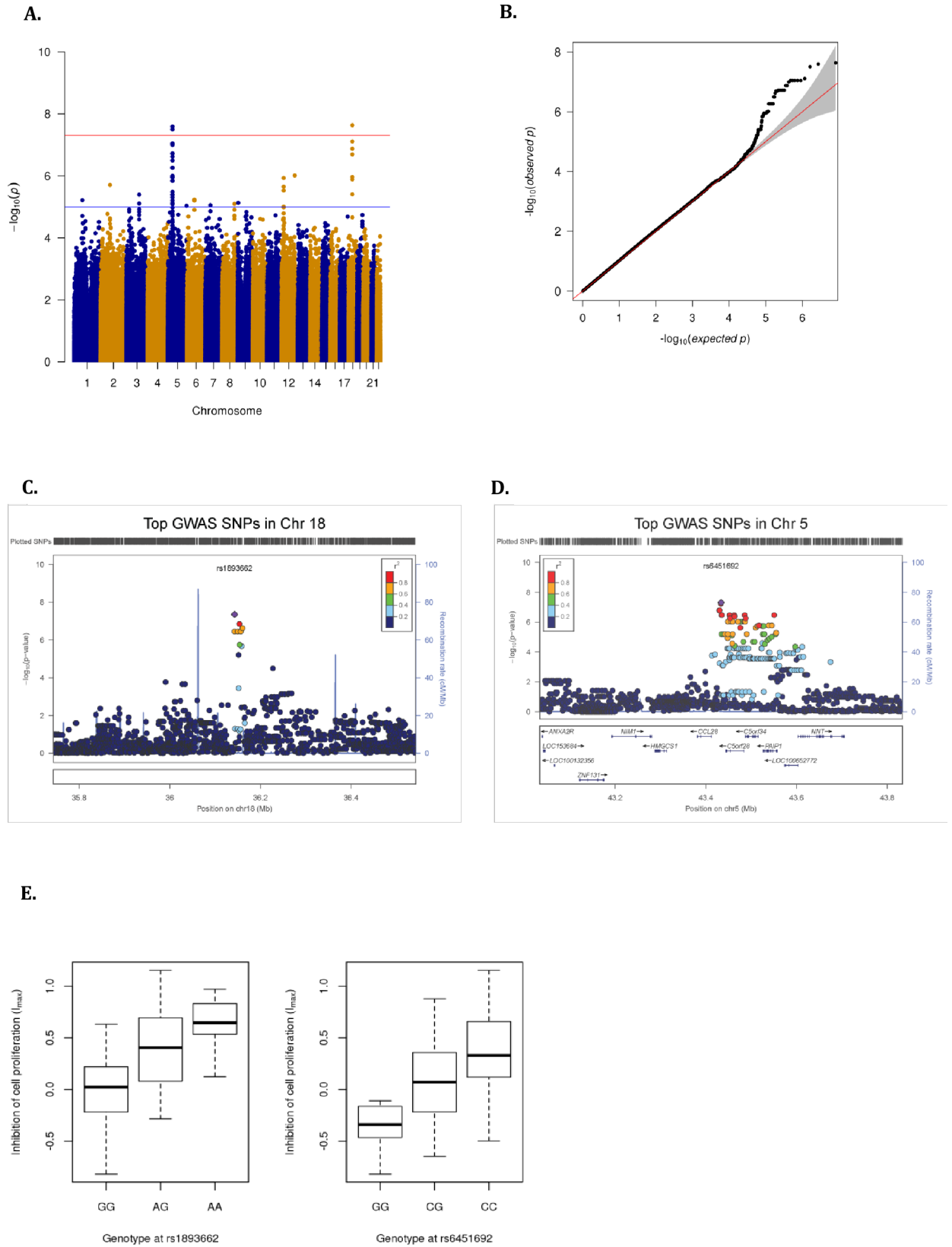


Fig 1. GWAS of inhibition of cellular proliferation by 1,25D (I_{\max}). (A) Manhattan plot of $-\log_{10}$ p-values of association of genome-wide variants with I_{\max} . (B) Quantile-quantile (QQ) plot of distribution of observed $-\log_{10}$ p-values on the y-axis, versus the expected $-\log_{10}$ p-values on the x-axis. LocusZoom plots of the I_{\max} GWAS associated regions in (C) chromosome 18 around rs1893662, and (D) chromosome 5 around rs6451692 (400kb windows, using 1000 genomes African populations as a reference). (E) Boxplots of I_{\max} relative to genotypes of rs1893662 and rs6451692. I_{\max} was corrected for age, gender, time of blood collection, batch, serum 25D levels, serum cortisol levels, and cell type proportions, and then fit to a normal distribution.

doi:10.1371/journal.pone.0159779.g001

Mapping Variation in Transcriptional Response to 1,25D

We measured the expression of 11,897 genes in PBMCs from 85 donors treated with 100nM 1,25D and vehicle for 6 hours. We identified 720 genes differentially expressed (DE) in response to 1,25D at a $FDR < 0.01$. Biological pathways significantly enriched among these genes included immune response pathways such as TREM1 signaling ($p = 4.0 \times 10^{-7}$, $FDR = 2 \times 10^{-4}$), Granulocyte differentiation and Diapedesis ($p = 2.0 \times 10^{-5}$, $FDR = 4 \times 10^{-3}$), and T Helper Cell Differentiation ($p = 6.0 \times 10^{-4}$, $FDR = 6.5 \times 10^{-2}$) (S7 Table), confirming the important role of 1,25D as an immunomodulator. In addition, there was an enrichment of the VDR/RXR activation pathway ($p = 7.0 \times 10^{-4}$, $FDR = 6.5 \times 10^{-2}$), including genes such as *CD14*, which encodes a monocyte surface antigen mediating innate immune response to bacterial lipopolysaccharide (LPS), *CAMP* which encodes an antimicrobial peptide, and *CYP24A1* which encodes the enzyme that initiates the degradation of 1,25D. A previous study characterizing patterns of transcriptional response to 1,25D and LPS in primary monocytes also found an overlapping list of immune response pathways identified in this study enriched among genes that were significantly down-regulated by 1,25D [57].

In order to identify polymorphisms that influence the transcriptional response to 1,25D, we tested the association between \log_2 fold change in transcript levels at each expressed gene and SNPs within 100kb of each gene using Matrix eQTL. Because DE genes tend to be those with consistent differences in transcript levels across all individuals, they may be biased against genes with common regulatory polymorphisms. For this reason, we did not limit our mapping analyses to the DE genes. We identified response *cis*-eQTLs for 8 genes at a $FDR < 0.10$, with the most significant response eQTLs including the transcriptional factor ets variant 3-line (*ETV3L*), and EH-domain containing 4 (*EHD4*), which plays a role in early endosomal transport (Table 1A, S6 Fig). Mapping \log_2 -fold change does not distinguish among the types of genotype-by-treatment interactions that influence transcriptional response. To do that, we applied a Bayesian statistical framework using the BRIdGE software, which compares different interaction models to each other and to a null model of no genotypic effect in both treatment conditions. We identified 4 genes with high confidence interactions (posterior probability of interaction > 0.7) between 1,25D treatment and SNP genotype; all these interaction eQTLs followed a 1,25D-only model, namely genotype has an effect on transcript levels in the 1,25D-treated aliquot but not in the control-treated one (Table 1B). These interaction eQTLs included the top 2 most significant response eQTLs that had been identified by mapping \log_2 fold change: *ETV3L* and *EHD4*. In addition, we identified interaction eQTLs in leucine rich repeat containing 25 (*LRRC25*), which is involved in activation of various immune cell types, and the transcriptional regulator unkempt family zinc finger (*UNK*).

To evaluate additional response *cis*-eQTLs found in VDR response elements, we identified 988 SNPs within VDR ChIP-seq peaks from a dataset of published THP-1 monocytic cell lines treated with 1,25D [49], and mapped response eQTLs using this subset of SNPs. At a distance of 1Mb, we identified statistically significant response eQTLs ($FDR < 0.10$) in two genes: FERM Domain Containing 6 (*FRMD6*), a key activator of the Hippo kinase pathway with important roles in regulating cell proliferation and apoptosis [58], and the undefined *KIAA1211* (Fig 2). In addition, we identified 17,417 SNPs within open chromatin regions,

Table 1. cis-eQTLs for transcriptional response to 1,25D.

(A) cis-eQTL mapping of log-fold change expression using Matrix eQTL					
SNP	Gene	T-Statistic	P-value	FDR	Beta
rs74116976	<i>ETV3L</i>	6.77	1.73×10^{-09}	1.17×10^{-4}	0.84
rs11070354	<i>EHD4</i>	6.11	3.16×10^{-8}	1.28×10^{-3}	0.86
rs7311057	<i>PARPBP</i>	5.73	1.56×10^{-7}	2.43×10^{-2}	0.79
rs59937851	<i>ZNHIT1</i>	5.41	5.98×10^{-7}	1.52×10^{-2}	1.02
rs7178702	<i>SPESP1</i>	5.12	1.97×10^{-6}	1.30×10^{-2}	0.69
rs10282056	<i>COBL</i>	-4.78	7.50×10^{-6}	3.10×10^{-2}	-0.92
rs62014366	<i>VWA9</i>	4.74	8.66×10^{-6}	4.67×10^{-2}	0.94
rs7779605	<i>CPED1</i>	4.31	4.38×10^{-5}	7.63×10^{-2}	0.75

(B) Interaction cis-eQTL mapping using BRIdGE					
Gene	SNP	Posterior probability for each interaction model			
		Control-only	1,25D-only	General interaction	No interaction
<i>EHD4</i>	rs1648856	0	0.994	0	0.001
<i>LRRC25</i>	rs3848646	0	0.965	0	0.027
<i>UNK</i>	rs8081606	0	0.803	0	0.049
<i>ETV3L</i>	rs6689823	0	0.723	0	0.277

doi:10.1371/journal.pone.0159779.t001

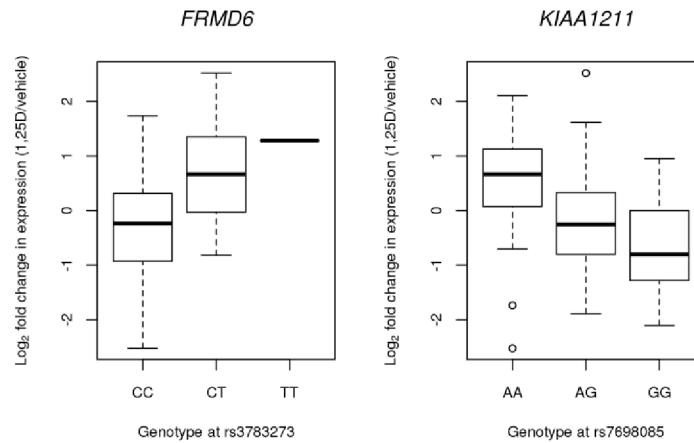
identified by FAIRE-seq from a published dataset of THP-1 monocytic cell lines treated with 1,25D [50]. Within this subset, we identified statistically significant response eQTLs (FDR < 0.10) in *ETV3L*, *EHD4* and *ZNHIT1* (S8 Table). These eQTLs were in strong linkage disequilibrium (LD) with the response eQTLs we had identified for the same genes ($r^2 = 0.93$, 0.69 and 0.95 for *ETV3L*, *EHD4* and *ZNHIT1*, respectively), raising the possibility that these response eQTLs are due to variants affecting open chromatin conformation.

Combined Analysis of Cellular and Transcriptional Response Phenotypes

We examined the relationship between the two 1,25D response phenotypes: transcriptional response and the inhibition of cellular proliferation. To evaluate whether the SNPs associated with inhibition of cellular proliferation exerted their effects through regulation of transcriptional response, we first examined associations between the two most significant I_{max} GWAS SNPs and \log_2 fold change expression at all 11,897 genes expressed in the PBMCs. At a FDR < 0.10, we found no statistically significant associations. We then focused on the subset of genes where \log_2 fold change in expression was associated with I_{max} , reasoning that these genes are more likely to share genetic variation influencing both transcriptional response and inhibition of cell proliferation. Using a linear regression approach, we identified 16 associated genes at an FDR < 0.2 (S9 Table). When we considered only these genes, we found significant associations between two I_{max} -associated genes (*PCSK6* and *RASL11A*) and the top GWAS SNP in chromosome 18, rs1893662, and one I_{max} -associated gene (*KNCN*) with the second GWAS SNP in chromosome 5, rs6451692 (Table 2), at a Bonferroni-corrected $p < 3.125 \times 10^{-3}$. Both *PCSK6* and *KNCN* are involved in vesicular trafficking and secretory pathways, highlighting potential molecular mechanisms involved in inhibition of proliferation by vitamin D.

We further predicted putative causal genes associated with I_{max} based on a Bayesian approach implemented in the program, Sherlock, using our response eQTL and GWAS of I_{max} data. At $p < 10^{-4}$ (FDR = 0.3), we identified three putative I_{max} -associated genes, including the translation initiation gene *PAIP1*, a transcriptional repressor gene *ZNF649*, and a golgin family gene *GORAB* (S10 Table). Interestingly, the top I_{max} -associated SNP in chromosome 5,

A.



B.

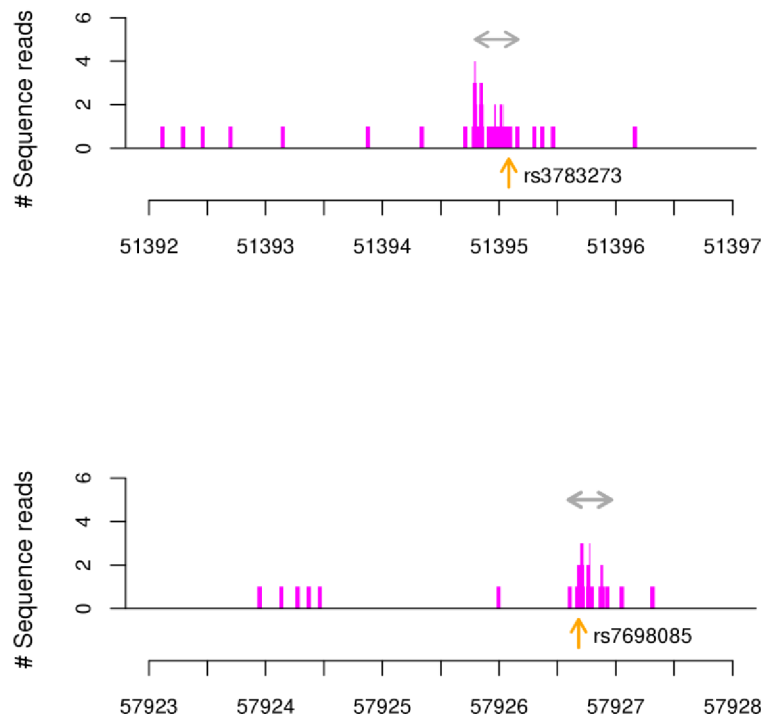


Fig 2. Associations between SNPs in vitamin D receptor (VDR) binding sites and transcriptional response. (A) Boxplots showing the effect of genotype on log₂ fold change of *FRMD6* and *KIAA1211* transcript levels, with genotypes of the associated SNPs on the x-axis. (B) Location of SNPs associated with transcription response of *FRMD6* (rs3783273, top panel) and *KIAA1211* (rs7698085, bottom panel) within VDR binding sites, indicated by the gray horizontal arrows. The SNP locations are indicated by the vertical orange arrows. VDR binding site information was obtained from a published ChIP-seq dataset from THP-1 monocytic cells treated with 1,25D and bacterial lipopolysaccharide (LPS).

doi:10.1371/journal.pone.0159779.g002

Table 2. Association between top I_{max} GWAS SNPs and transcriptional response.

Gene Name	rs1893662		rs6451692	
	Beta	P-value	Beta	P-value
<i>PCSK6</i>	-2.09	2.1×10^{-3}	-0.78	0.26
<i>SMARCD3</i>	2.01	2.1×10^{-3}	0.93	0.16
<i>RASL11A</i>	2.08	2.3×10^{-3}	1.17	0.09
<i>KNCN</i>	-1.24	3.21×10^{-2}	-1.85	9.95×10^{-4}

doi:10.1371/journal.pone.0159779.t002

rs6451692, was identified as being associated with transcriptional response of *PAIP1* using this method, which suggests that this SNP influences the inhibition of cell proliferation through a transcriptional mechanism in PBMCs.

Discussion

While the inter-individual variation in the circulating inactive form of vitamin D, 25D, has been well documented, little is known about the inter-individual variation in immune response to the active 1,25D. In this study, we identified several variants underlying variation in response to 1,25D both at the cellular and transcriptional level using primary peripheral blood mononuclear cells from a cohort of healthy individuals of African-American ancestry. These variants highlight genes with an important role in mediating the immunomodulatory effects of 1,25D, thereby providing a genetic basis for inter-individual variation in those aspects of the immune response influenced by vitamin D.

Intergenic SNPs in chromosome 5 that were significantly associated with inhibition of cellular proliferation by 1,25D are located close to several genes such as *CCL28*, which encodes a chemokine that recruits T cells, eosinophils, and B cells to mucosal sites [59–61], and *PAIP1* which encodes a protein that interacts with poly(A)-binding protein and with the eIF4A cap-binding complex, stimulating translation initiation [62]. Interestingly, we found a marginal association between rs6451692 and down-regulation of *PAIP1*, raising the possibility that this polymorphism influences the inhibitory effects of 1,25D on immune cell proliferation by regulating the transcriptional response of a translation initiation gene.

We observed several regulatory marks near rs6451692 in seven cell lines from the ENCODE project, including an enrichment of H3K4me1 histone mark, which is associated with enhancers. There was also an abundance of transcription factor binding events in this region, where rs6451692 overlaps a TCF7L2 binding site. TCF7L2 is a member of the high mobility group DNA binding protein family of transcription factors which has been implicated in type 2 diabetes risk [63–65]. Other transcription factors with binding sites in the region include RXRA, which binds to the VDR, forming a heterodimer which then regulates transcription of vitamin D-responsive genes, GATA3 which has important roles in T cell development [66, 67], and CEBPB which plays an important role in regulating immune and inflammatory response genes [68–71]. The abundance of transcription factor binding events in this region suggests that the regulatory activity of rs6451692 on the surrounding genes could involve enhancer activity. Further functional validation assays specifically in PBMCs treated with vitamin D are needed to elucidate the regulatory mechanisms of this I_{max} GWAS interval.

In addition, from the Genotype-Tissue Expression (GTEx) project catalogue [72], we observed that rs6451692 is associated with variation in transcript levels of surrounding genes in multiple tissues. The C allele is associated with decreased expression of *CCL28* in the pancreas, decreased expression of *NNT* in skeletal muscle, and decreased expression of the novel antisense long non-coding RNA *RP11-159F24.5* in multiple tissues such as subcutaneous

adipose, tibial nerve, testis, thyroid and skin, suggesting that this variant influences the regulation of several genes in that genomic region. *RP11-159F24.5* was not covered by probes in our expression microarrays, therefore we cannot determine if rs6451692 has effects on the expression of this gene in PBMCs.

Enrichment of immune response pathways such as TREM1 signaling, which enhances innate immune responses to microbial infections and activates pro-inflammatory responses [73], and T helper cell differentiation among the genes that respond transcriptionally to 1,25D, underscores the important immunomodulatory role played by 1,25D [8–10]. This is consistent with results from previous studies from our group investigating the transcriptional response to 1,25D in PBMCs [39] and transcriptional response to 1,25D and bacterial lipopolysaccharide (LPS) in primary monocytes [57]. Both of these studies found an enrichment of immune response pathways, particularly among genes that were down-regulated by 1,25D. This highlights the important immunomodulatory role played by 1,25D across cells in both the innate and adaptive immune system. In addition, translation initiation pathways were significantly enriched among the genes that were up-regulated by 1,25D in monocytes in the previous study. This pathway was not significantly enriched amongst the DE genes in PBMCs in this study (S7 Table), which could indicate that this effect is particularly strong in the innate immune cells. It was however interesting to note the marginal association between one of the top I_{\max} SNPs, rs6451692, and transcriptional response of *PAIP1*, a translation initiation gene.

Several studies have mapped genome-wide VDR binding sites in different immune cell lines [49, 74, 75]. Interestingly, one study examined VDR binding sites in primary CD4⁺ T cells from nine individuals with varying 25D levels and reported a correlation between 25D levels and number of VDR binding sites [76], directly supporting the notion that vitamin D status affects the response to vitamin D. In addition, genome-wide maps of VDR binding sites allow identification of genetic variants within VDR binding sites that in turn may influence variation in the transcriptional response to vitamin D. Interestingly, one such study reported that many risk variants for autoimmune diseases detected in genome-wide association studies fall within VDR binding sites [70], suggesting that disease risk is influenced not only by inter-individual variation in 25D levels, but also by variation in the response to vitamin D. To build on these studies, we focused on mapping variants that regulate genome-wide transcriptional response to 1,25D in primary PBMCs. The *cis*-response eQTLs identified in this study highlighted several genes that could play an important role in mediating the effects of 1,25D in the immune response. Genes identified using both the linear regression and Bayesian eQTL mapping approaches included *ETV3L*, which is a transcriptional regulator that has been reported to play a role in inhibiting proliferation of neural progenitor cells [77], and *EHD4*, which plays a role in controlling early endosomal trafficking [78, 79]. Furthermore, we identified statistically significant response eQTLs in regions of open chromatin, marked by FAIRE-seq peaks in *ETV3L*, *EHD4*, and *ZNHIT1*—a gene that is implicated in regulating the transcriptional activity of the orphan nuclear receptor Rev-erbeta [80]. Interestingly, both *ETV3L* and *ZNHIT1* are transcriptional regulators, raising the possibility that these loci could play a role in modulating transcriptional response of other genes to 1,25D in immune cells.

We then identified variants within VDR binding sites that regulate transcriptional response possibly by altering the structure or accessibility of the VDR binding site. We did this by combining our *cis*-response eQTL data with a published VDR ChIP-seq dataset from a monocytic cell line [49]. We identified a response eQTL within a VDR binding site in *FRMD6*, which is part of the conserved Hippo pathway playing a critical role in controlling organ size by regulating both cell proliferation and apoptosis [81, 82]. *FRMD6* has been linked to various complex diseases such as asthma, Alzheimer's disease, and lung cancer [82–84], where it is thought to have tumor suppressor properties. The T allele of rs3783273, which is associated with increased

FRMD6 expression (Fig 2), could alter the binding properties of the VDR to its receptor elements in *FRMD6* and could affect the transcriptional response of this gene to 1,25D. Given its putative tumor suppressor properties, *FRMD6* may play a crucial role in mediating the role of 1,25D in inhibiting proliferation of immune cells.

The published VDR ChIP-seq and FAIRE-seq data were collected in a monocytic cell line stimulated with LPS and treated with 1,25D. Our data, in contrast, were collected in a heterogeneous population of immune cells treated with PHA, which was shown to stimulate transcriptional responses related to both innate and adaptive immunity [38]. Therefore, the data from the monocytic cell line may miss some peaks specific to other cell types present in PBMCs, that is, primarily T cells, but it may also contribute valuable information about the regulatory architecture of 1,25D response in immune cells. Future work should incorporate VDR ChIP-seq and FAIRE-seq studies in primary immune cells under the same experimental conditions.

Using both simple linear regression analysis and a Bayesian approach, we combined the information from response *cis*-eQTL mapping and the GWAS of I_{\max} to identify candidate genes mediating the inhibitory effects of cellular proliferation by 1,25D. Genes such as *PAIP1*, *ZNF649* and *GORAB* contained I_{\max} -associated SNPs that also regulated transcriptional response of these genes in *cis*. While *PAIP1* encodes a protein that is involved in initiating translation, *ZNF649* encodes a transcriptional repressor that inhibits transcription factor complexes such as AP-1 which is involved in cellular proliferation and survival [85–87], and *GORAB* encodes a golgin family member with roles in the intracellular membrane trafficking and the secretory pathways of the Golgi apparatus [88, 89]. In addition, we identified *trans* effects of the top GWAS SNPs on transcriptional response of genes such as *PCSK6* and *KNCN*, which both have roles in vesicular trafficking and secretory pathways, highlighting potential molecular mechanisms involved in the anti-proliferative activity of 1,25D. Increased *PCSK6* expression has been previously implicated in risk for rheumatoid arthritis [90]. Interestingly, knockdown of *PCSK6* by RNA interference significantly decreased proliferation, invasion, and migration of cultured rheumatoid arthritis synovial fibroblasts. It is plausible that the top I_{\max} -associated SNP, rs1893662, regulates the anti-proliferative activity of 1,25D by regulating *PCSK6* transcription in immune cells. The potential mechanisms through which these putative I_{\max} -associated candidate genes could mediate the inhibition of proliferation of immune cells by 1,25D should be further studied.

In summary, mapping response to 1,25D at both the cellular and transcriptional level in immune cells enabled identification of variants which may influence inter-individual variation in response to 1,25D, and identification of genes with potentially crucial roles in mediating the immunomodulatory role of 1,25D. Characterizing these genetic mediators of 1,25D activity in the immune system could inform additional therapeutic targets and markers for immune-related diseases in future randomized VD supplementation trials.

Supporting Information

S1 Fig. Experimental Design. Peripheral blood mononuclear cells (PBMCs) were obtained from 88 healthy African American donors. PBMCs were cultured for 6 hours with phytohemagglutinin (PHA) and either vehicle (EtOH) or 1,25-dihydroxyvitamin D3 (1,25D), and RNA was extracted for gene expression measurements. PBMCs from the same samples were also cultured for 48 hours with PHA and either vehicle or 1,25D for cell proliferation measurements. DNA was also extracted from PBMCs for genotyping. (DOCX)

S2 Fig. Correlation between serum 25D levels and African ancestry proportions. Serum levels of 25D are negatively correlated with global proportions of African ancestry. Serum 25D

levels were corrected for age and batch effects.
(DOCX)

S3 Fig. Distribution of raw counts per minute (CPM) across genotypes at the top I_{\max} GWAS SNPs. rs1893662 is at the top panel, and rs6451692 is at the bottom panel. Boxplots of CPM in 1,25D treatment, vehicle control, and in the ratio of 1,25D to vehicle, are colored in blue, pink and green respectively.
(DOCX)

S4 Fig. Global distribution of allele frequencies. The allele frequency distribution across global populations of the top I_{\max} GWAS SNPs, (A) rs1893662 and (B) rs6451692. Image obtained from the Geography of Genetic Variants (GGV) browser [91].
(DOCX)

S5 Fig. Magnified view of the I_{\max} GWAS interval in chromosome 5. The location of rs6451692 is highlighted by the blue rectangle. Nearby enhancer marks (H3K4me1), DNase I hypersensitive sites, and transcription factor binding sites were obtained from seven cell lines from the ENCODE project [56].
(DOCX)

S6 Fig. Results from 1,25D response *cis*-eQTL mapping using Matrix eQTL [46]. Boxplots show the effect of genotype on \log_2 fold change in transcript levels of 8 genes, with genotype coded as the number of copies of the minor allele. All SNPs are within 100kb of the transcriptional start site (TSS) of their respective genes.
(DOCX)

S1 Table. Subject characteristics, sample collection times and cell type composition.
(XLSX)

S2 Table. Cell proliferation measurements. Counts per minute (CPM) measurements in 1,25D treatment and in vehicle control, and I_{\max} values for all samples.
(XLSX)

S3 Table. Gene expression values and differential expression analysis results. Normalized \log_2 -expression values per individual and per treatment for 11,897 genes, and differential expression results from paired t-test comparing expression in 1,25D-treated samples to expression in vehicle-treated samples.
(XLSX)

S4 Table. Correlation between I_{\max} and covariates. The association between I_{\max} and sample covariates was tested using a simple linear regression, indicating that there were no significant associations between I_{\max} and the covariates ($p > 0.05$).
(DOCX)

S5 Table. The top SNPs identified in the GWAS of I_{\max} . The SNPs shown have p-values $< 1 \times 10^{-8}$, which corresponds to a FDR of 0.036.
(DOCX)

S6 Table. Association between top I_{\max} -associated SNPs in chromosome 5, and transcription response of nearby genes (within 100kb).
(DOCX)

S7 Table. Gene set enrichment analysis of significantly differentially expressed (DE) genes (FDR < 0.01), using Ingenuity Pathway Analysis (IPA) software. Enriched pathways shown

are at a p-value threshold of 0.05. The top 8 pathways were statistically significant at a FDR < 0.10. B-H p-value* = Benjamini-Hochberg multiple testing corrected p-value. (DOCX)

S8 Table. Response *cis*-eQTLs found in open chromatin regions detected by FAIRE-seq.

These response eQTLs are significant at a FDR < 0.10. The strength of the FAIRE-seq peaks is indicated by the Peak p-values and FDR, as well as the Peak fold enrichment values. (DOCX)

S9 Table. Genes whose transcription responses are associated with I_{\max} at a FDR < 0.2.

(DOCX)

S10 Table. Putative I_{\max} -associated genes. Genes associated with I_{\max} were detected using a Bayesian approach implemented in the statistical program Sherlock [54]. The strength of the association between the genes and I_{\max} is given by the overall \log_{10} of Bayes factor (LBF).

(DOCX)

S11 Table. List of loci highlighted in this study, and their respective phenotypic associations reported in the GWAS catalogue [92].

(DOCX)

Acknowledgments

The authors are grateful to Xin He, Marcelo Nobrega, Sonia Kupfer, Nicholas Knoblauch, John Blischak, and the entire Di Rienzo lab for helpful discussions about the project.

Author Contributions

Conceived and designed the experiments: ADR JCM. Performed the experiments: JCM SSB. Analyzed the data: SNK CJ SN CLH DBW. Contributed reagents/materials/analysis tools: AIS ADR. Wrote the paper: SNK ADR.

References

1. Correale J, Ysraelit MC, Gaitan MI. Immunomodulatory effects of Vitamin D in multiple sclerosis. *Brain*. 2009; 132(Pt 5):1146–60. Epub 2009/03/27. doi: [10.1093/brain/awp033](https://doi.org/10.1093/brain/awp033) PMID: [19321461](https://pubmed.ncbi.nlm.nih.gov/19321461/).
2. Pakpoor J, Ramagopalan S. Evidence for an Association Between Vitamin D and Multiple Sclerosis. *Curr Top Behav Neurosci*. 2015; 26:105–15. Epub 2014/12/17. doi: [10.1007/7854_2014_358](https://doi.org/10.1007/7854_2014_358) PMID: [25502544](https://pubmed.ncbi.nlm.nih.gov/25502544/).
3. Ascherio A, Munger KL, Simon KC. Vitamin D and multiple sclerosis. *Lancet Neurol*. 2010; 9(6):599–612. Epub 2010/05/25. doi: [10.1016/s1474-4422\(10\)70086-7](https://doi.org/10.1016/s1474-4422(10)70086-7) PMID: [20494325](https://pubmed.ncbi.nlm.nih.gov/20494325/).
4. Hypponen E, Laara E, Reunanen A, Jarvelin MR, Virtanen SM. Intake of vitamin D and risk of type 1 diabetes: a birth-cohort study. *Lancet*. 2001; 358(9292):1500–3. Epub 2001/11/14. doi: [10.1016/s0140-6736\(01\)06580-1](https://doi.org/10.1016/s0140-6736(01)06580-1) PMID: [11705562](https://pubmed.ncbi.nlm.nih.gov/11705562/).
5. Kamen DL, Cooper GS, Bouali H, Shaftman SR, Hollis BW, Gilkeson GS. Vitamin D deficiency in systemic lupus erythematosus. *Autoimmun Rev*. 2006; 5(2):114–7. Epub 2006/01/25. doi: [10.1016/j.autrev.2005.05.009](https://doi.org/10.1016/j.autrev.2005.05.009) PMID: [16431339](https://pubmed.ncbi.nlm.nih.gov/16431339/).
6. Kamen D, Aranow C. Vitamin D in systemic lupus erythematosus. *Curr Opin Rheumatol*. 2008; 20(5):532–7. Epub 2008/08/14. doi: [10.1097/BOR.0b013e32830a991b](https://doi.org/10.1097/BOR.0b013e32830a991b) PMID: [18698173](https://pubmed.ncbi.nlm.nih.gov/18698173/).
7. Deluca HF, Cantorna MT. Vitamin D: its role and uses in immunology. *Faseb j*. 2001; 15(14):2579–85. Epub 2001/12/01. doi: [10.1096/fj.01-0433rev](https://doi.org/10.1096/fj.01-0433rev) PMID: [11726533](https://pubmed.ncbi.nlm.nih.gov/11726533/).
8. Baeke F, Takiishi T, Korf H, Gysemans C, Mathieu C. Vitamin D: modulator of the immune system. *Curr Opin Pharmacol*. 2010; 10(4):482–96. Epub 2010/04/30. doi: [10.1016/j.coph.2010.04.001](https://doi.org/10.1016/j.coph.2010.04.001) PMID: [20427238](https://pubmed.ncbi.nlm.nih.gov/20427238/).
9. Aranow C. Vitamin D and the immune system. *J Investig Med*. 2011; 59(6):881–6. Epub 2011/04/30. doi: [10.2311/JIM.0b013e31821b8755](https://doi.org/10.2311/JIM.0b013e31821b8755) PMID: [21527855](https://pubmed.ncbi.nlm.nih.gov/21527855/); PubMed Central PMCID: PMC3166406.

10. Peelen E, Knippenberg S, Muris AH, Thewissen M, Smolders J, Tervaert JW, et al. Effects of vitamin D on the peripheral adaptive immune system: a review. *Autoimmun Rev*. 2011; 10(12):733–43. Epub 2011/05/31. doi: [10.1016/j.autrev.2011.05.002](https://doi.org/10.1016/j.autrev.2011.05.002) PMID: [21621002](https://pubmed.ncbi.nlm.nih.gov/21621002/).
11. Bikle D. Nonclassic actions of vitamin D. *J Clin Endocrinol Metab*. 2009; 94(1):26–34. Epub 2008/10/16. doi: [10.1210/jc.2008-1454](https://doi.org/10.1210/jc.2008-1454) PMID: [18854395](https://pubmed.ncbi.nlm.nih.gov/18854395/); PubMed Central PMCID: [PMCPmc2630868](https://pubmed.ncbi.nlm.nih.gov/PMC/PMC2630868/).
12. Lin R, White JH. The pleiotropic actions of vitamin D. *Bioessays*. 2004; 26(1):21–8. Epub 2003/12/30. doi: [10.1002/bies.10368](https://doi.org/10.1002/bies.10368) PMID: [14696037](https://pubmed.ncbi.nlm.nih.gov/14696037/).
13. Ramagopalan SV, Dymont DA, Cader MZ, Morrison KM, Disanto G, Morahan JM, et al. Rare variants in the CYP27B1 gene are associated with multiple sclerosis. *Ann Neurol*. 2011; 70(6):881–6. Epub 2011/12/23. doi: [10.1002/ana.22678](https://doi.org/10.1002/ana.22678) PMID: [22190362](https://pubmed.ncbi.nlm.nih.gov/22190362/).
14. Genome-wide association study identifies new multiple sclerosis susceptibility loci on chromosomes 12 and 20. *Nat Genet*. 2009; 41(7):824–8. Epub 2009/06/16. doi: [10.1038/ng.396](https://doi.org/10.1038/ng.396) PMID: [19525955](https://pubmed.ncbi.nlm.nih.gov/19525955/).
15. Sawcer S, Hellenthal G, Pirinen M, Spencer CC, Patsopoulos NA, Moutsianas L, et al. Genetic risk and a primary role for cell-mediated immune mechanisms in multiple sclerosis. *Nature*. 2011; 476(7359):214–9. Epub 2011/08/13. doi: [10.1038/nature10251](https://doi.org/10.1038/nature10251) PMID: [21833088](https://pubmed.ncbi.nlm.nih.gov/21833088/); PubMed Central PMCID: [PMCPMC3182531](https://pubmed.ncbi.nlm.nih.gov/PMC/PMC3182531/).
16. Christakos S, Dhawan P, Liu Y, Peng X, Porta A. New insights into the mechanisms of vitamin D action. *J Cell Biochem*. 2003; 88(4):695–705. Epub 2003/02/11. doi: [10.1002/jcb.10423](https://doi.org/10.1002/jcb.10423) PMID: [12577303](https://pubmed.ncbi.nlm.nih.gov/12577303/).
17. Ben-Zvi I, Aranow C, Mackay M, Stanevsky A, Kamen DL, Marinescu LM, et al. The impact of vitamin D on dendritic cell function in patients with systemic lupus erythematosus. *PLoS One*. 2010; 5(2):e9193. Epub 2010/02/20. doi: [10.1371/journal.pone.0009193](https://doi.org/10.1371/journal.pone.0009193) PMID: [20169063](https://pubmed.ncbi.nlm.nih.gov/20169063/); PubMed Central PMCID: [PMCPmc2821911](https://pubmed.ncbi.nlm.nih.gov/PMC/PMC2821911/).
18. Ferreira GB, Vanherwegen AS, Eelen G, Gutierrez AC, Van Lommel L, Marchal K, et al. Vitamin D3 Induces Tolerance in Human Dendritic Cells by Activation of Intracellular Metabolic Pathways. *Cell Rep*. 2015. Epub 2015/02/11. doi: [10.1016/j.celrep.2015.01.013](https://doi.org/10.1016/j.celrep.2015.01.013) PMID: [25660022](https://pubmed.ncbi.nlm.nih.gov/25660022/).
19. Rigby WF, Waugh MG. Decreased accessory cell function and costimulatory activity by 1,25-dihydroxyvitamin D3-treated monocytes. *Arthritis Rheum*. 1992; 35(1):110–9. Epub 1992/01/01. PMID: [1370618](https://pubmed.ncbi.nlm.nih.gov/1370618/).
20. Lemire JM, Adams JS, Sakai R, Jordan SC. 1 alpha,25-dihydroxyvitamin D3 suppresses proliferation and immunoglobulin production by normal human peripheral blood mononuclear cells. *J Clin Invest*. 1984; 74(2):657–61. Epub 1984/08/01. doi: [10.1172/jci111465](https://doi.org/10.1172/jci111465) PMID: [6611355](https://pubmed.ncbi.nlm.nih.gov/6611355/); PubMed Central PMCID: [PMCPMC370520](https://pubmed.ncbi.nlm.nih.gov/PMC/PMC370520/).
21. Lemire JM, Adams JS, Kermani-Arab V, Bakke AC, Sakai R, Jordan SC. 1,25-Dihydroxyvitamin D3 suppresses human T helper/inducer lymphocyte activity in vitro. *J Immunol*. 1985; 134(5):3032–5. Epub 1985/05/01. PMID: [3156926](https://pubmed.ncbi.nlm.nih.gov/3156926/).
22. Jeffery LE, Burke F, Mura M, Zheng Y, Qureshi OS, Hewison M, et al. 1,25-Dihydroxyvitamin D3 and IL-2 combine to inhibit T cell production of inflammatory cytokines and promote development of regulatory T cells expressing CTLA-4 and FoxP3. *J Immunol*. 2009; 183(9):5458–67. Epub 2009/10/22. doi: [10.4049/jimmunol.0803217](https://doi.org/10.4049/jimmunol.0803217) PMID: [19843932](https://pubmed.ncbi.nlm.nih.gov/19843932/); PubMed Central PMCID: [PMCPMC2810518](https://pubmed.ncbi.nlm.nih.gov/PMC/PMC2810518/).
23. Chen S, Sims GP, Chen XX, Gu YY, Lipsky PE. Modulatory effects of 1,25-dihydroxyvitamin D3 on human B cell differentiation. *J Immunol*. 2007; 179(3):1634–47. Epub 2007/07/21. PMID: [17641030](https://pubmed.ncbi.nlm.nih.gov/17641030/).
24. Looker AC, Johnson CL, Lacher DA, Pfeiffer CM, Schleicher RL, Sempos CT. Vitamin D status: United States, 2001–2006. *NCHS Data Brief*. 2011;(59):1–8. PMID: [21592422](https://pubmed.ncbi.nlm.nih.gov/21592422/).
25. Freedman BI, Register TC. Effect of race and genetics on vitamin D metabolism, bone and vascular health. *Nat Rev Nephrol*. 2012; 8(8):459–66. Epub 2012/06/13. doi: [10.1038/nmeph.2012.112](https://doi.org/10.1038/nmeph.2012.112) PMID: [22688752](https://pubmed.ncbi.nlm.nih.gov/22688752/).
26. Rostand SG. Vitamin D, blood pressure, and African Americans: toward a unifying hypothesis. *Clin J Am Soc Nephrol*. 2010; 5(9):1697–703. Epub 2010/07/24. doi: [10.2215/cjn.02960410](https://doi.org/10.2215/cjn.02960410) PMID: [20651156](https://pubmed.ncbi.nlm.nih.gov/20651156/).
27. Murphy AB, Kelley B, Nyame YA, Martin IK, Smith DJ, Castaneda L, et al. Predictors of serum vitamin D levels in African American and European American men in Chicago. *Am J Mens Health*. 2012; 6(5):420–6. Epub 2012/03/09. doi: [10.1177/1557988312437240](https://doi.org/10.1177/1557988312437240) PMID: [22398989](https://pubmed.ncbi.nlm.nih.gov/22398989/); PubMed Central PMCID: [PMCPmc3678722](https://pubmed.ncbi.nlm.nih.gov/PMC/PMC3678722/).
28. Jostins L, Ripke S, Weersma RK, Duerr RH, McGovern DP, Hui KY, et al. Host-microbe interactions have shaped the genetic architecture of inflammatory bowel disease. *Nature*. 2012; 491(7422):119–24. Epub 2012/11/07. doi: [10.1038/nature11582](https://doi.org/10.1038/nature11582) PMID: [23128233](https://pubmed.ncbi.nlm.nih.gov/23128233/); PubMed Central PMCID: [PMCPMC3491803](https://pubmed.ncbi.nlm.nih.gov/PMC/PMC3491803/).
29. Wang TJ, Zhang F, Richards JB, Kestenbaum B, van Meurs JB, Berry D, et al. Common genetic determinants of vitamin D insufficiency: a genome-wide association study. *Lancet*. 2010; 376(9736):180–8.

- Epub 2010/06/15. doi: [10.1016/s0140-6736\(10\)60588-0](https://doi.org/10.1016/s0140-6736(10)60588-0) PMID: [20541252](https://pubmed.ncbi.nlm.nih.gov/20541252/); PubMed Central PMCID: [PMCPMC3086761](https://pubmed.ncbi.nlm.nih.gov/pmc/articles/PMC3086761/).
30. Smolders J, Peelen E, Thewissen M, Cohen Tervaert JW, Menheere P, Hupperts R, et al. Safety and T cell modulating effects of high dose vitamin D3 supplementation in multiple sclerosis. *PLoS One*. 2010; 5(12):e15235. Epub 2010/12/24. doi: [10.1371/journal.pone.0015235](https://doi.org/10.1371/journal.pone.0015235) PMID: [21179201](https://pubmed.ncbi.nlm.nih.gov/21179201/); PubMed Central PMCID: [PMCPMC3001453](https://pubmed.ncbi.nlm.nih.gov/pmc/articles/PMC3001453/).
 31. Prietl B, Pilz S, Wolf M, Tomaschitz A, Obermayer-Pietsch B, Graninger W, et al. Vitamin D supplementation and regulatory T cells in apparently healthy subjects: vitamin D treatment for autoimmune diseases? *Isr Med Assoc J*. 2010; 12(3):136–9. Epub 2010/08/06. PMID: [20684175](https://pubmed.ncbi.nlm.nih.gov/20684175/).
 32. Wejse C, Gomes VF, Rabna P, Gustafson P, Aaby P, Lisse IM, et al. Vitamin D as supplementary treatment for tuberculosis: a double-blind, randomized, placebo-controlled trial. *Am J Respir Crit Care Med*. 2009; 179(9):843–50. Epub 2009/01/31. doi: [10.1164/rccm.200804-567OC](https://doi.org/10.1164/rccm.200804-567OC) PMID: [19179490](https://pubmed.ncbi.nlm.nih.gov/19179490/).
 33. Li-Ng M, Aloia JF, Pollack S, Cunha BA, Mikhail M, Yeh J, et al. A randomized controlled trial of vitamin D3 supplementation for the prevention of symptomatic upper respiratory tract infections. *Epidemiol Infect*. 2009; 137(10):1396–404. Epub 2009/03/20. doi: [10.1017/s0950268809002404](https://doi.org/10.1017/s0950268809002404) PMID: [19296870](https://pubmed.ncbi.nlm.nih.gov/19296870/).
 34. Martineau AR, Wilkinson RJ, Wilkinson KA, Newton SM, Kampmann B, Hall BM, et al. A single dose of vitamin D enhances immunity to mycobacteria. *Am J Respir Crit Care Med*. 2007; 176(2):208–13. Epub 2007/04/28. doi: [10.1164/rccm.200701-007OC](https://doi.org/10.1164/rccm.200701-007OC) PMID: [17463418](https://pubmed.ncbi.nlm.nih.gov/17463418/).
 35. Aloia JF, Patel M, Dimaano R, Li-Ng M, Talwar SA, Mikhail M, et al. Vitamin D intake to attain a desired serum 25-hydroxyvitamin D concentration. *Am J Clin Nutr*. 2008; 87(6):1952–8. Epub 2008/06/11. PMID: [18541590](https://pubmed.ncbi.nlm.nih.gov/18541590/).
 36. Zhao LJ, Zhou Y, Bu F, Travers-Gustafson D, Ye A, Xu X, et al. Factors predicting vitamin D response variation in non-Hispanic white postmenopausal women. *J Clin Endocrinol Metab*. 2012; 97(8):2699–705. Epub 2012/05/16. doi: [10.1210/jc.2011-3401](https://doi.org/10.1210/jc.2011-3401) PMID: [22585090](https://pubmed.ncbi.nlm.nih.gov/22585090/); PubMed Central PMCID: [PMCPMC3410260](https://pubmed.ncbi.nlm.nih.gov/pmc/articles/PMC3410260/).
 37. Martineau AR, Timms PM, Bothamley GH, Hanifa Y, Islam K, Claxton AP, et al. High-dose vitamin D(3) during intensive-phase antimicrobial treatment of pulmonary tuberculosis: a double-blind randomised controlled trial. *Lancet*. 2011; 377(9761):242–50. Epub 2011/01/11. doi: [10.1016/s0140-6736\(10\)61889-2](https://doi.org/10.1016/s0140-6736(10)61889-2) PMID: [21215445](https://pubmed.ncbi.nlm.nih.gov/21215445/); PubMed Central PMCID: [PMCPMC4176755](https://pubmed.ncbi.nlm.nih.gov/pmc/articles/PMC34176755/).
 38. Maranville JC, Baxter SS, Witonsky DB, Chase MA, Di Rienzo A. Genetic mapping with multiple levels of phenotypic information reveals determinants of lymphocyte glucocorticoid sensitivity. *Am J Hum Genet*. 2013; 93(4):735–43. Epub 2013/09/24. doi: [10.1016/j.ajhg.2013.08.005](https://doi.org/10.1016/j.ajhg.2013.08.005) PMID: [24055111](https://pubmed.ncbi.nlm.nih.gov/24055111/); PubMed Central PMCID: [PMCPMC3791266](https://pubmed.ncbi.nlm.nih.gov/pmc/articles/PMC3791266/).
 39. Kupfer SS, Maranville JC, Baxter SS, Huang Y, Di Rienzo A. Comparison of cellular and transcriptional responses to 1,25-dihydroxyvitamin d3 and glucocorticoids in peripheral blood mononuclear cells. *PLoS One*. 2013; 8(10):e76643. Epub 2013/10/12. doi: [10.1371/journal.pone.0076643](https://doi.org/10.1371/journal.pone.0076643) PMID: [24116131](https://pubmed.ncbi.nlm.nih.gov/24116131/); PubMed Central PMCID: [PMCPmc3792986](https://pubmed.ncbi.nlm.nih.gov/pmc/articles/PMC3792986/).
 40. Maranville JC, Baxter SS, Torres JM, Di Rienzo A. Inter-ethnic differences in lymphocyte sensitivity to glucocorticoids reflect variation in transcriptional response. *Pharmacogenomics J*. 2013; 13(2):121–9. Epub 2011/12/14. doi: [10.1038/tpj.2011.55](https://doi.org/10.1038/tpj.2011.55) PMID: [22158329](https://pubmed.ncbi.nlm.nih.gov/22158329/); PubMed Central PMCID: [PMCPmc3774530](https://pubmed.ncbi.nlm.nih.gov/pmc/articles/PMC3774530/).
 41. Du P, Kibbe WA, Lin SM. lumi: a pipeline for processing Illumina microarray. *Bioinformatics*. 2008; 24(13):1547–8. Epub 2008/05/10. doi: [10.1093/bioinformatics/btn224](https://doi.org/10.1093/bioinformatics/btn224) PMID: [18467348](https://pubmed.ncbi.nlm.nih.gov/18467348/).
 42. Storey JD, Tibshirani R. Statistical significance for genomewide studies. *Proc Natl Acad Sci U S A*. 2003; 100(16):9440–5. Epub 2003/07/29. doi: [10.1073/pnas.1530509100](https://doi.org/10.1073/pnas.1530509100) PMID: [12883005](https://pubmed.ncbi.nlm.nih.gov/12883005/); PubMed Central PMCID: [PMCPmc170937](https://pubmed.ncbi.nlm.nih.gov/pmc/articles/PMC170937/).
 43. Abecasis GR, Auton A, Brooks LD, DePristo MA, Durbin RM, Handsaker RE, et al. An integrated map of genetic variation from 1,092 human genomes. *Nature*. 2012; 491(7422):56–65. Epub 2012/11/07. doi: [10.1038/nature11632](https://doi.org/10.1038/nature11632) PMID: [23128226](https://pubmed.ncbi.nlm.nih.gov/23128226/); PubMed Central PMCID: [PMCPMC3498066](https://pubmed.ncbi.nlm.nih.gov/pmc/articles/PMC3498066/).
 44. Howie BN, Donnelly P, Marchini J. A flexible and accurate genotype imputation method for the next generation of genome-wide association studies. *PLoS Genet*. 2009; 5(6):e1000529. Epub 2009/06/23. doi: [10.1371/journal.pgen.1000529](https://doi.org/10.1371/journal.pgen.1000529) PMID: [19543373](https://pubmed.ncbi.nlm.nih.gov/19543373/); PubMed Central PMCID: [PMCPMC2689936](https://pubmed.ncbi.nlm.nih.gov/pmc/articles/PMC2689936/).
 45. Pritchard JK, Stephens M, Donnelly P. Inference of population structure using multilocus genotype data. *Genetics*. 2000; 155(2):945–59. Epub 2000/06/03. PMID: [10835412](https://pubmed.ncbi.nlm.nih.gov/10835412/); PubMed Central PMCID: [PMCPMC1461096](https://pubmed.ncbi.nlm.nih.gov/pmc/articles/PMC1461096/).
 46. Shabalín AA. Matrix eQTL: ultra fast eQTL analysis via large matrix operations. *Bioinformatics*. 2012; 28(10):1353–8. Epub 2012/04/12. doi: [10.1093/bioinformatics/bts163](https://doi.org/10.1093/bioinformatics/bts163) PMID: [22492648](https://pubmed.ncbi.nlm.nih.gov/22492648/); PubMed Central PMCID: [PMCPMC3348564](https://pubmed.ncbi.nlm.nih.gov/pmc/articles/PMC3348564/).

47. Benjamini Y, Hochberg Y. Controlling the False Discovery Rate: A Practical and Powerful Approach to Multiple Testing.
48. Maranville JC, Luca F, Richards AL, Wen X, Witonsky DB, Baxter S, et al. Interactions between glucocorticoid treatment and cis-regulatory polymorphisms contribute to cellular response phenotypes. *PLoS Genet.* 2011; 7(7):e1002162. Epub 2011/07/14. doi: [10.1371/journal.pgen.1002162](https://doi.org/10.1371/journal.pgen.1002162) PMID: [21750684](https://pubmed.ncbi.nlm.nih.gov/21750684/); PubMed Central PMCID: PMCPmc3131293.
49. Tuoresmaki P, Vaisanen S, Neme A, Heikkinen S, Carlberg C. Patterns of genome-wide VDR locations. *PLoS One.* 2014; 9(4):e96105. Epub 2014/05/03. doi: [10.1371/journal.pone.0096105](https://doi.org/10.1371/journal.pone.0096105) PMID: [24787735](https://pubmed.ncbi.nlm.nih.gov/24787735/); PubMed Central PMCID: PMCPmc4005760.
50. Seuter S, Heikkinen S, Carlberg C. Chromatin acetylation at transcription start sites and vitamin D receptor binding regions relates to effects of 1alpha,25-dihydroxyvitamin D3 and histone deacetylase inhibitors on gene expression. *Nucleic Acids Res.* 2013; 41(1):110–24. Epub 2012/10/25. doi: [10.1093/nar/gks959](https://doi.org/10.1093/nar/gks959) PMID: [23093607](https://pubmed.ncbi.nlm.nih.gov/23093607/); PubMed Central PMCID: PMCPmc3592476.
51. Li H, Handsaker B, Wysoker A, Fennell T, Ruan J, Homer N, et al. The Sequence Alignment/Map format and SAMtools. *Bioinformatics.* 2009; 25(16):2078–9. Epub 2009/06/10. doi: [10.1093/bioinformatics/btp352](https://doi.org/10.1093/bioinformatics/btp352) PMID: [19505943](https://pubmed.ncbi.nlm.nih.gov/19505943/); PubMed Central PMCID: PMCPMC2723002.
52. Landt SG, Marinov GK, Kundaje A, Kheradpour P, Pauli F, Batzoglu S, et al. ChIP-seq guidelines and practices of the ENCODE and modENCODE consortia. *Genome Res.* 2012; 22(9):1813–31. Epub 2012/09/08. doi: [10.1101/gr.136184.111](https://doi.org/10.1101/gr.136184.111) PMID: [22955991](https://pubmed.ncbi.nlm.nih.gov/22955991/); PubMed Central PMCID: PMCPMC3431496.
53. Zhang Y, Liu T, Meyer CA, Eeckhoutte J, Johnson DS, Bernstein BE, et al. Model-based analysis of ChIP-Seq (MACS). *Genome Biol.* 2008; 9(9):R137. Epub 2008/09/19. doi: [10.1186/gb-2008-9-9-r137](https://doi.org/10.1186/gb-2008-9-9-r137) PMID: [18798982](https://pubmed.ncbi.nlm.nih.gov/18798982/); PubMed Central PMCID: PMCPMC2592715.
54. He X, Fuller CK, Song Y, Meng Q, Zhang B, Yang X, et al. Sherlock: detecting gene-disease associations by matching patterns of expression QTL and GWAS. *Am J Hum Genet.* 2013; 92(5):667–80. Epub 2013/05/07. doi: [10.1016/j.ajhg.2013.03.022](https://doi.org/10.1016/j.ajhg.2013.03.022) PMID: [23643380](https://pubmed.ncbi.nlm.nih.gov/23643380/); PubMed Central PMCID: PMCPMC3644637.
55. Io Medicine. Dietary reference intakes for calcium and vitamin D. Washington (DC): National Academies Press; 2011.
56. An integrated encyclopedia of DNA elements in the human genome. *Nature.* 2012; 489(7414):57–74. Epub 2012/09/08. doi: [10.1038/nature11247](https://doi.org/10.1038/nature11247) PMID: [22955616](https://pubmed.ncbi.nlm.nih.gov/22955616/); PubMed Central PMCID: PMCPMC3439153.
57. Kariuki SN, Blischak JD, Nakagome S, Witonsky DB, Di Rienzo A. Patterns of transcriptional response to 1,25-dihydroxyvitamin D3 and bacterial lipopolysaccharide in primary human monocytes. *bioRxiv.* 2015. doi: [10.1101/030759](https://doi.org/10.1101/030759).
58. Angus L, Moleirinho S, Herron L, Sinha A, Zhang X, Nestrata M, et al. Willin/FRMD6 expression activates the Hippo signaling pathway kinases in mammals and antagonizes oncogenic YAP. *Oncogene.* 2012; 31(2):238–50. Epub 2011/06/15. doi: [10.1038/onc.2011.224](https://doi.org/10.1038/onc.2011.224) PMID: [21666719](https://pubmed.ncbi.nlm.nih.gov/21666719/).
59. Wang W, Soto H, Oldham ER, Buchanan ME, Homey B, Catron D, et al. Identification of a novel chemokine (CCL28), which binds CCR10 (GPR2). *J Biol Chem.* 2000; 275(29):22313–23. Epub 2000/04/27. doi: [10.1074/jbc.M001461200](https://doi.org/10.1074/jbc.M001461200) PMID: [10781587](https://pubmed.ncbi.nlm.nih.gov/10781587/).
60. Pan J, Kunkel EJ, Gosslar U, Lazarus N, Langdon P, Broadwell K, et al. A novel chemokine ligand for CCR10 and CCR3 expressed by epithelial cells in mucosal tissues. *J Immunol.* 2000; 165(6):2943–9. Epub 2000/09/07. PMID: [10975800](https://pubmed.ncbi.nlm.nih.gov/10975800/).
61. Hieshima K, Ohtani H, Shibano M, Izawa D, Nakayama T, Kawasaki Y, et al. CCL28 has dual roles in mucosal immunity as a chemokine with broad-spectrum antimicrobial activity. *J Immunol.* 2003; 170(3):1452–61. Epub 2003/01/23. PMID: [12538707](https://pubmed.ncbi.nlm.nih.gov/12538707/).
62. Craig AW, Haghhighat A, Yu AT, Sonenberg N. Interaction of polyadenylate-binding protein with the eIF4G homologue PAIP enhances translation. *Nature.* 1998; 392(6675):520–3. Epub 1998/04/21. doi: [10.1038/33198](https://doi.org/10.1038/33198) PMID: [9548260](https://pubmed.ncbi.nlm.nih.gov/9548260/).
63. Grant SF, Thorleifsson G, Reynisdottir I, Benediktsson R, Manolescu A, Sainz J, et al. Variant of transcription factor 7-like 2 (TCF7L2) gene confers risk of type 2 diabetes. *Nat Genet.* 2006; 38(3):320–3. Epub 2006/01/18. doi: [10.1038/ng1732](https://doi.org/10.1038/ng1732) PMID: [16415884](https://pubmed.ncbi.nlm.nih.gov/16415884/).
64. Cauchi S, El Achhab Y, Choquet H, Dina C, Kremler F, Weitgasser R, et al. TCF7L2 is reproducibly associated with type 2 diabetes in various ethnic groups: a global meta-analysis. *J Mol Med (Berl).* 2007; 85(7):777–82. Epub 2007/05/04. doi: [10.1007/s00109-007-0203-4](https://doi.org/10.1007/s00109-007-0203-4) PMID: [17476472](https://pubmed.ncbi.nlm.nih.gov/17476472/).
65. Savic D, Ye H, Aneas I, Park SY, Bell GI, Nobrega MA. Alterations in TCF7L2 expression define its role as a key regulator of glucose metabolism. *Genome Res.* 2011; 21(9):1417–25. Epub 2011/06/16. doi: [10.1101/gr.123745.111](https://doi.org/10.1101/gr.123745.111) PMID: [21673050](https://pubmed.ncbi.nlm.nih.gov/21673050/); PubMed Central PMCID: PMCPMC3166827.

66. Wei G, Abraham BJ, Yagi R, Jothi R, Cui K, Sharma S, et al. Genome-wide analyses of transcription factor GATA3-mediated gene regulation in distinct T cell types. *Immunity*. 2011; 35(2):299–311. Epub 2011/08/27. doi: [10.1016/j.immuni.2011.08.007](https://doi.org/10.1016/j.immuni.2011.08.007) PMID: [21867929](https://pubmed.ncbi.nlm.nih.gov/21867929/); PubMed Central PMCID: PMCPMC3169184.
67. Ho IC, Tai TS, Pai SY. GATA3 and the T-cell lineage: essential functions before and after T-helper-2-cell differentiation. *Nat Rev Immunol*. 2009; 9(2):125–35. Epub 2009/01/20. doi: [10.1038/nri2476](https://doi.org/10.1038/nri2476) PMID: [19151747](https://pubmed.ncbi.nlm.nih.gov/19151747/); PubMed Central PMCID: PMCPMC2998182.
68. Akira S, Isshiki H, Sugita T, Tanabe O, Kinoshita S, Nishio Y, et al. A nuclear factor for IL-6 expression (NF-IL6) is a member of a C/EBP family. *Embo j*. 1990; 9(6):1897–906. Epub 1990/06/01. PMID: [2112087](https://pubmed.ncbi.nlm.nih.gov/2112087/); PubMed Central PMCID: PMCPMC551896.
69. Pope RM, Leutz A, Ness SA. C/EBP beta regulation of the tumor necrosis factor alpha gene. *J Clin Invest*. 1994; 94(4):1449–55. Epub 1994/10/01. doi: [10.1172/jci117482](https://doi.org/10.1172/jci117482) PMID: [7929820](https://pubmed.ncbi.nlm.nih.gov/7929820/); PubMed Central PMCID: PMCPMC295278.
70. Wedel A, Sulski G, Ziegler-Heitbrock HW. CCAAT/enhancer binding protein is involved in the expression of the tumour necrosis factor gene in human monocytes. *Cytokine*. 1996; 8(5):335–41. Epub 1996/05/01. PMID: [8726660](https://pubmed.ncbi.nlm.nih.gov/8726660/).
71. Poli V. The role of C/EBP isoforms in the control of inflammatory and native immunity functions. *J Biol Chem*. 1998; 273(45):29279–82. Epub 1998/10/29. PMID: [9792624](https://pubmed.ncbi.nlm.nih.gov/9792624/).
72. The Genotype-Tissue Expression (GTEx) project. *Nat Genet*. 2013; 45(6):580–5. Epub 2013/05/30. doi: [10.1038/ng.2653](https://doi.org/10.1038/ng.2653) PMID: [23715323](https://pubmed.ncbi.nlm.nih.gov/23715323/); PubMed Central PMCID: PMCPMC4010069.
73. Colonna M, Facchetti F. TREM-1 (triggering receptor expressed on myeloid cells): a new player in acute inflammatory responses. *J Infect Dis*. 2003; 187 Suppl 2:S397–401. Epub 2003/06/07. doi: [10.1086/374754](https://doi.org/10.1086/374754) PMID: [12792857](https://pubmed.ncbi.nlm.nih.gov/12792857/).
74. Ramagopalan SV, Heger A, Berlanga AJ, Maugeri NJ, Lincoln MR, Burrell A, et al. A ChIP-seq defined genome-wide map of vitamin D receptor binding: associations with disease and evolution. *Genome Res*. 2010; 20(10):1352–60. Epub 2010/08/26. doi: [10.1101/gr.107920.110](https://doi.org/10.1101/gr.107920.110) PMID: [20736230](https://pubmed.ncbi.nlm.nih.gov/20736230/); PubMed Central PMCID: PMCPMC2945184.
75. Heikkinen S, Vaisanen S, Pehkonen P, Seuter S, Benes V, Carlberg C. Nuclear hormone 1alpha,25-dihydroxyvitamin D3 elicits a genome-wide shift in the locations of VDR chromatin occupancy. *Nucleic Acids Res*. 2011; 39(21):9181–93. Epub 2011/08/19. doi: [10.1093/nar/gkr654](https://doi.org/10.1093/nar/gkr654) PMID: [21846776](https://pubmed.ncbi.nlm.nih.gov/21846776/); PubMed Central PMCID: PMCPMC3241659.
76. Handel AE, Sandve GK, Disanto G, Berlanga-Taylor AJ, Gallone G, Hanwell H, et al. Vitamin D receptor ChIP-seq in primary CD4+ cells: relationship to serum 25-hydroxyvitamin D levels and autoimmune disease. *BMC Med*. 2013; 11:163. Epub 2013/07/16. doi: [10.1186/1741-7015-11-163](https://doi.org/10.1186/1741-7015-11-163) PMID: [23849224](https://pubmed.ncbi.nlm.nih.gov/23849224/); PubMed Central PMCID: PMCPMC3710212.
77. Janesick A, Abbey R, Chung C, Liu S, Taketani M, Blumberg B. ERF and ETV3L are retinoic acid-inducible repressors required for primary neurogenesis. *Development*. 2013; 140(15):3095–106. Epub 2013/07/05. doi: [10.1242/dev.093716](https://doi.org/10.1242/dev.093716) PMID: [23824578](https://pubmed.ncbi.nlm.nih.gov/23824578/).
78. George M, Ying G, Rainey MA, Solomon A, Parikh PT, Gao Q, et al. Shared as well as distinct roles of EHD proteins revealed by biochemical and functional comparisons in mammalian cells and *C. elegans*. *BMC Cell Biol*. 2007; 8:3. Epub 2007/01/20. doi: [10.1186/1471-2121-8-3](https://doi.org/10.1186/1471-2121-8-3) PMID: [17233914](https://pubmed.ncbi.nlm.nih.gov/17233914/); PubMed Central PMCID: PMCPMC1793994.
79. Sharma M, Naslavsky N, Caplan S. A role for EHD4 in the regulation of early endosomal transport. *Traffic*. 2008; 9(6):995–1018. Epub 2008/03/12. doi: [10.1111/j.1600-0854.2008.00732.x](https://doi.org/10.1111/j.1600-0854.2008.00732.x) PMID: [18331452](https://pubmed.ncbi.nlm.nih.gov/18331452/); PubMed Central PMCID: PMCPMC2795359.
80. Wang J, Li Y, Zhang M, Liu Z, Wu C, Yuan H, et al. A zinc finger HIT domain-containing protein, ZNHIT-1, interacts with orphan nuclear hormone receptor Rev-erbeta and removes Rev-erbeta-induced inhibition of apoCIII transcription. *Febs j*. 2007; 274(20):5370–81. Epub 2007/09/26. doi: [10.1111/j.1742-4658.2007.06062.x](https://doi.org/10.1111/j.1742-4658.2007.06062.x) PMID: [17892483](https://pubmed.ncbi.nlm.nih.gov/17892483/).
81. Zhao B, Li L, Lei Q, Guan KL. The Hippo-YAP pathway in organ size control and tumorigenesis: an updated version. *Genes Dev*. 2010; 24(9):862–74. Epub 2010/05/05. doi: [10.1101/gad.1909210](https://doi.org/10.1101/gad.1909210) PMID: [20439427](https://pubmed.ncbi.nlm.nih.gov/20439427/); PubMed Central PMCID: PMCPMC2861185.
82. Ungvari I, Hullam G, Antal P, Kiszal PS, Gezi A, Hadadi E, et al. Evaluation of a partial genome screening of two asthma susceptibility regions using bayesian network based bayesian multilevel analysis of relevance. *PLoS One*. 2012; 7(3):e33573. Epub 2012/03/21. doi: [10.1371/journal.pone.0033573](https://doi.org/10.1371/journal.pone.0033573) PMID: [22432035](https://pubmed.ncbi.nlm.nih.gov/22432035/); PubMed Central PMCID: PMCPMC3303848.
83. Hong MG, Reynolds CA, Feldman AL, Kallin M, Lambert JC, Amouyel P, et al. Genome-wide and gene-based association implicates FRMD6 in Alzheimer disease. *Hum Mutat*. 2012; 33(3):521–9. Epub 2011/12/23. doi: [10.1002/humu.22009](https://doi.org/10.1002/humu.22009) PMID: [22190428](https://pubmed.ncbi.nlm.nih.gov/22190428/); PubMed Central PMCID: PMCPMC3326347.

84. Zhang R, Chu M, Zhao Y, Wu C, Guo H, Shi Y, et al. A genome-wide gene-environment interaction analysis for tobacco smoke and lung cancer susceptibility. *Carcinogenesis*. 2014; 35(7):1528–35. Epub 2014/03/25. doi: [10.1093/carcin/bgu076](https://doi.org/10.1093/carcin/bgu076) PMID: [24658283](https://pubmed.ncbi.nlm.nih.gov/24658283/); PubMed Central PMCID: PMCPMC4076813.
85. Yang H, Yuan W, Wang Y, Zhu C, Liu B, Yang D, et al. ZNF649, a novel Kruppel type zinc-finger protein, functions as a transcriptional suppressor. *Biochem Biophys Res Commun*. 2005; 333(1):206–15. Epub 2005/06/14. doi: [10.1016/j.bbrc.2005.05.101](https://doi.org/10.1016/j.bbrc.2005.05.101) PMID: [15950191](https://pubmed.ncbi.nlm.nih.gov/15950191/).
86. Karin M, Liu Z, Zandi E. AP-1 function and regulation. *Curr Opin Cell Biol*. 1997; 9(2):240–6. Epub 1997/04/01. PMID: [9069263](https://pubmed.ncbi.nlm.nih.gov/9069263/).
87. Shaulian E, Karin M. AP-1 as a regulator of cell life and death. *Nat Cell Biol*. 2002; 4(5):E131–6. Epub 2002/05/04. doi: [10.1038/ncb0502-e131](https://doi.org/10.1038/ncb0502-e131) PMID: [11988758](https://pubmed.ncbi.nlm.nih.gov/11988758/).
88. Egerer J, Emmerich D, Fischer-Zirnsak B, Chan WL, Meierhofer D, Tuysuz B, et al. GORAB Missense Mutations Disrupt RAB6 and ARF5 Binding and Golgi Targeting. *J Invest Dermatol*. 2015; 135(10):2368–76. Epub 2015/05/23. doi: [10.1038/jid.2015.192](https://doi.org/10.1038/jid.2015.192) PMID: [26000619](https://pubmed.ncbi.nlm.nih.gov/26000619/).
89. Yildirim Y, Tolun A, Tuysuz B. The phenotype caused by PYCR1 mutations corresponds to geroderma osteodysplasticum rather than autosomal recessive cutis laxa type 2. *Am J Med Genet A*. 2011; 155a(1):134–40. Epub 2011/01/05. doi: [10.1002/ajmg.a.33747](https://doi.org/10.1002/ajmg.a.33747) PMID: [21204221](https://pubmed.ncbi.nlm.nih.gov/21204221/).
90. Wang F, Wang L, Jiang H, Chang X, Pan J. Inhibition of PCSK6 may play a protective role in the development of rheumatoid arthritis. *J Rheumatol*. 2015; 42(2):161–9. Epub 2014/12/01. doi: [10.3899/jrheum.140435](https://doi.org/10.3899/jrheum.140435) PMID: [25433529](https://pubmed.ncbi.nlm.nih.gov/25433529/).
91. Marcus J, Novembre J. Geography of Genetic Variants (GGV) v0.1. Available: <http://www.popgen.uchicago/ggv/>.
92. Welter D, MacArthur J, Morales J, Burdett T, Hall P, Junkins H, et al. The NHGRI GWAS Catalog, a curated resource of SNP-trait associations. *Nucleic Acids Res*. 2014; 42(Database issue):D1001–6. Epub 2013/12/10. doi: [10.1093/nar/gkt1229](https://doi.org/10.1093/nar/gkt1229) PMID: [24316577](https://pubmed.ncbi.nlm.nih.gov/24316577/); PubMed Central PMCID: PMCPMC3965119.